

# Mode-Locked $\text{Ho}^{3+}$ -Doped ZBLAN Fiber Laser at $1.2 \mu\text{m}$

Xuezhong Yang, Lei Zhang, Yan Feng, Xiushan Zhu, R. A. Norwood, and N. Peyghambarian

**Abstract**—A mode-locked  $\text{Ho}^{3+}$ -doped ZBLAN fiber laser at  $1.2 \mu\text{m}$  was demonstrated for the first time employing a nonlinear polarization rotation technique for mode-locking. The laser was pumped at  $1137 \text{ nm}$  by the Raman fiber laser. Stable dissipative soliton mode-locking was achieved with an intracavity Lyot filter formed from a length of polarization maintaining fiber and a polarization dependent optical isolator.  $1.3\text{-nJ}$  pulses with pulse duration of  $47 \text{ ps}$  at a repetition rate of  $1.77 \text{ MHz}$  were produced. Multiple pulse operation with burst energy up to  $6.7 \text{ nJ}$  was observed at higher pump power.

**Index Terms**—Fiber laser, Holmium doped ZBLAN fiber, Lyot filter, mode locked, nonlinear polarization rotation (NPR).

## I. INTRODUCTION

**R**OBUST and compact fiber lasers operating in the  $1.2 \mu\text{m}$  region have found a variety of applications in molecular spectroscopy, photodynamic therapy, biomedical diagnostics, oxygen atmospheric sensing, laser guide star adaptive optics, etc. [1]–[5]. Raman fiber lasers and Bismuth doped fiber lasers have been used to produce laser emissions in this wavelength region [4]–[8]. However, their unit gains are small and very long gain fibers are required. Holmium ( $\text{Ho}^{3+}$ )-doped  $\text{ZrF}_4\text{-BaF}_2\text{-LaF}_3\text{-AlF}_3\text{-NaF}$  (ZBLAN) fibers have been demonstrated as a high-efficiency gain medium for  $1.2 \mu\text{m}$  lasers owing to the low phonon energy and long radiative lifetimes of rare-earth-doped ZBLAN [9], [10]. Because of the high unit gain of  $\text{Ho}^{3+}$ -doped ZBLAN fiber, a single-frequency all-fiber laser at  $1200 \text{ nm}$  with a linewidth less than  $100 \text{ kHz}$  has been demonstrated with a distributed Bragg reflector configuration [11]. Moreover, a  $2.4 \text{ W}$   $1190 \text{ nm}$  all-fiber laser with a slope efficiency of  $42\%$  was recently achieved with just a  $10 \text{ cm}$  long  $\text{Ho}^{3+}$ -doped ZBLAN fiber [12]. Most recently, Liu *et al.* reported a graphene Q-switched  $\text{Ho}^{3+}$ -doped

ZBLAN fiber laser at  $1190 \text{ nm}$  with a pulse duration of  $0.8 \mu\text{s}$  and pulse energy of  $0.44 \text{ nJ}$  at a repetition rate of  $111 \text{ kHz}$  [9]. Compared to Q-switched lasers, mode-locked lasers usually can provide much shorter pulses with much higher peak powers at higher repetition rates, which are in great demand for various applications. However, to the best of our knowledge, there has been no reported mode-locked  $\text{Ho}^{3+}$ -doped ZBLAN fiber laser at  $1.2 \mu\text{m}$ .

In this letter, we report a mode-locked  $\text{Ho}^{3+}$ -doped ZBLAN fiber laser at  $1.2 \mu\text{m}$  for the first time. The nonlinear polarization rotation (NPR) technique was used to provide an artificial saturable absorption effect and mode lock the ring fiber laser. An all-fiber intra-cavity Lyot filter based on a length of polarization maintaining (PM) fiber and a polarization dependent isolator (ISO) was inserted into the all-normal-dispersion cavity to shape the mode-locked pulses and stabilize the dissipative solitons. Stable single-pulse mode-locking with a pulse energy of  $1 \text{ nJ}$  was obtained for various cavity lengths. Multi-pulse mode-locked operation was also observed at high pump power.

## II. EXPERIMENTAL SETUP

Besides absorption lines in the visible wavelength region,  $\text{Ho}^{3+}$ : ZBLAN has an absorption band around  $1150 \text{ nm}$ , corresponding to the transition from the ground state to the  $^5\text{I}_6$  level. Transition from the  $^5\text{I}_6$  level to the ground state generates the  $1.2 \mu\text{m}$  emission [11]. Pumping directly into the upper laser level has the advantage of a low quantum defect and therefore reduced thermal load. In our experiment, the gain fiber was a  $12.5 \text{ cm}$  long  $3 \text{ mol}\%$   $\text{Ho}^{3+}$ -doped ZBLAN fiber, which has a core diameter of  $5.3 \mu\text{m}$ , core numerical aperture (NA) of  $0.14$ , and a cladding diameter of  $125 \mu\text{m}$ . The active fiber is a custom-designed fiber that was fabricated by IR Photonics. HI1060 silica fibers were spliced with the ZBLAN fiber at both ends with splice losses less than  $0.5 \text{ dB}$ , which was accomplished by Vytran FFS-2000 using the NP Photonics proprietary splicing technique [13]. A home-made linearly polarized Raman fiber laser at  $1137 \text{ nm}$  was used as the pump source. The configuration of the mode-locked ring fiber laser is depicted in Fig. 1. The pump laser was coupled into the ring resonator through a fused-type wavelength division multiplexer (WDM). Unidirectional operation of the ring laser was implemented by a polarization dependent isolator with the fast axis blocked, which also acts as an in-line polarizer. The propagation directions of the pump and signal light are opposite. A PM fiber coupler, which was designed as an  $1120/1178 \text{ nm}$  WDM, was utilized to extract most of the residual pump ( $>90\%$ ) and deliver  $20\%$  of the mode-locked laser out at  $1190 \text{ nm}$  as well. A short length of PM980 fiber was spliced with the PM fiber coupler at an angle of

Manuscript received March 29, 2016; revised June 21, 2016; accepted July 24, 2016. Date of publication August 9, 2016; date of current version September 2, 2016. This work was supported in part by National Natural Science Foundation of China under Grant 61378026 and Technology Research Initiative Fund Photonics Initiative of University of Arizona.

X. Yang is with the Shanghai Key Laboratory of Solid-State Lasers and Applications, Shanghai Institute of Optics and Fine Mechanics, Chinese Academy of Sciences, Shanghai 201800, China, and also with the University of the Chinese Academy of Sciences, Beijing 100049, China (e-mail: yangxuezhong000@163.com).

L. Zhang, and Y. Feng are with the Shanghai Key Laboratory of Solid-State Lasers and Applications, Shanghai Institute of Optics and Fine Mechanics, Chinese Academy of Sciences, Shanghai 201800, China (e-mail: zhangl@siom.ac.cn; feng@siom.ac.cn).

X. Zhu, R. A. Norwood, and N. Peyghambarian are with the College of Optical Sciences, University of Arizona, Tucson, AZ 85721 USA (e-mail: xszhu@email.arizona.edu; rnorwood@optics.arizona.edu; Nasser@optics.arizona.edu).

Color versions of one or more of the figures in this paper are available online at <http://ieeexplore.ieee.org>.

Digital Object Identifier 10.1109/JLT.2016.2599007

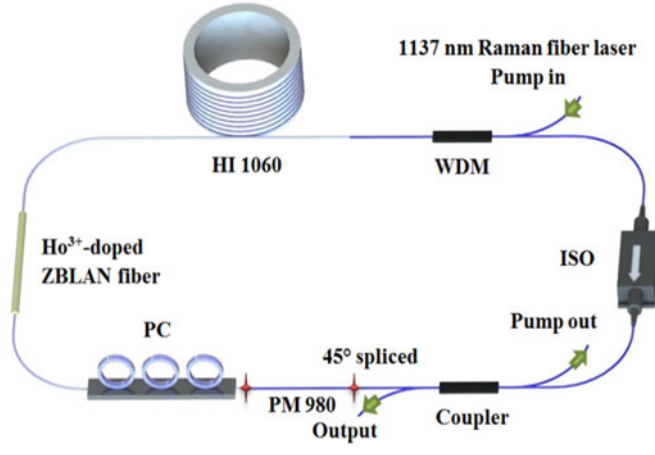


Fig. 1. Experimental configuration of the mode-locked Ho<sup>3+</sup>-doped ZBLAN fiber laser.

45° to form an all-fiber artificial Lyot filter, in which the polarization dependent isolator works as a polarizer and the PM980 fiber works as a waveplate [14]. A polarization controller (PC) was used to adjust the polarization state inside the ring cavity to tune the center wavelength of the Lyot filter and achieve mode-locked performance of the ring laser as well. The Ho<sup>3+</sup>-doped ZBLAN fiber was sandwiched between the PC and a long length of HI1060 fiber, which was used to adjust the total cavity length. The fiber cavity is all-normal dispersion at 1.2 μm and the total dispersion is determined by the long piece of HI1060 fiber, whose dispersion parameter  $D$  is about  $-10$  ps/(km·nm) at 1.2 μm. In the experiment, the output power was measured with a power meter (THORLABS, S145C). The pulse train was recorded (THORLABS, DET01CFC) and analyzed with a 1-GHz digital phosphor oscilloscope. The frequency spectrum of the mode-locked laser was recorded by a radio-frequency (RF) spectrum analyzer (KEYSIGHT, N9020A). The pulse width was measured with a background free autocorrelator (PulseCheck, SM1200, Scan range 2.1-1200 ps) and the optical spectrum of the laser was measured with an optical spectrum analyzer (YOKOGAWA, AQ6370B) having a resolution of 0.02 nm.

It is known that spectral filtering is required for pulse shaping and to achieve dissipative soliton mode-locking in an all normal dispersion cavity [15], [16]. Fiber-based Lyot filter with the advantages of high flexibility, easy implementation, and robust operation has been used in several all-normal-dispersion mode-locked fiber lasers [14], [17]–[19]. In our experimental setup, the light transmitted through the PM isolator is linearly polarized and propagates along the slow axis of the output PM fiber and the PM fiber coupler. Because the output fiber of the PM fiber coupler is spliced with the short length PM fiber segment at 45°, the linearly polarized light is coupled into two polarization states along the fast and slow axes of the PM fiber with equal amplitude. Due to the birefringence of the PM fiber, the accumulated phase difference between the two polarization states,  $\Delta\varphi$ , is given by  $\Delta\varphi = (2\pi/\lambda)L\Delta n$  [14], where  $L$  is the length of the PM fiber segment,  $\lambda$  is the wavelength of the light, and  $\Delta n$  is the birefringence of the PM fiber. The combination of the

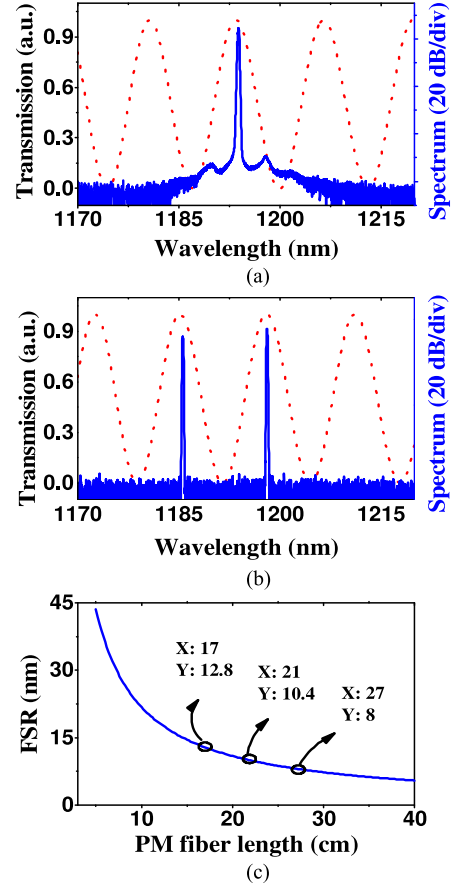


Fig. 2. (a) Single wavelength operation of the fiber ring laser. (b) Typical optical spectrum (solid blue curve) of dual wavelength operation of the fiber ring laser and the simulated transmission of the Lyot filter (dotted red curve). (c) Measured FSR of the Lyot filter for 17, 21, and 27 cm PM fibers and the calculated FSR of the Lyot filter as a function of PM fiber length.

PM isolator and the PM fiber segment forms an all-fiber Lyot filter and its transmission,  $T$ , is  $\cos^2(\Delta\varphi/2) = \cos^2(\pi L\Delta n/\lambda)$  [20], showing that the transmission of a Lyot filter is quasi-periodic in wavelength with a free spectral range (FSR) given by  $\Delta\lambda \sim \lambda^2/L\Delta n$  [14]. Thus, the bandwidth of a Lyot filter can be tailored by changing the length of the PM fiber segment. In the experiment, the polarization controller, the gain fiber, and the long piece of HI1060 fiber were spliced in serial between the PM fiber segment and the PM WDM. These non-PM fibers and fiber components contribute to the polarization rotation and the center wavelength of the Lyot filter can be tuned by changing the state of the polarization controller. Therefore, a wavelength tunable Lyot filter is formed in the fiber ring laser.

### III. RESULTS AND DISCUSSION

Tunable filtering of the artificial Lyot filter was confirmed by the continuous wave (CW) operation of the fiber ring laser at different wavelengths. Fig. 2(a) shows a single wavelength operation of the laser at 1193 nm, which is the transmission peak of the Lyot filter. When the polarization controller was tuned, dual wavelength operation of the laser was obtained as shown in Fig. 2(b), indicating that the transmission peaks of the Lyot filter

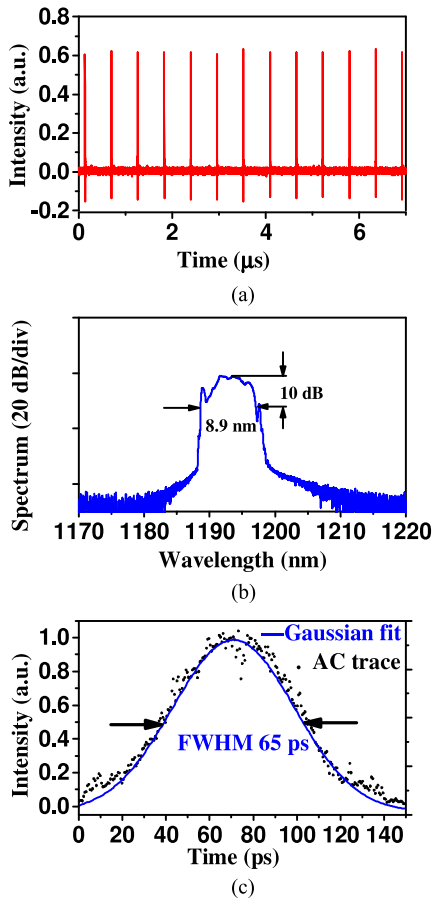


Fig. 3. (a) Pulse train, (b) output spectrum, and (c) autocorrelation trace of the mode-locked laser at a pump power of 900 mW.

can be shifted by changing the polarization state of the laser in the non-PM fibers. The wavelength separation between the two peaks is the FSR of the Lyot filter, which can be changed by using PM fibers with different lengths. When the HI1060 fiber was 100 m, for three different PM fiber lengths, namely 17, 21, and 27 cm, the peak to peak separation was measured to be 12.5, 10, and 7.4 nm, which are very close to the theoretical values of 12.8, 10.4, and 8 nm, respectively, as shown in Fig. 2(c). The slight deviation may be caused by uncertainties in the PM fiber length or the birefringence  $\Delta n(6.5 \times 10^{-4})$ .

The laser was mode-locked using NPR technique, which transforms intensity dependent polarization rotation into intensity modulation through the polarizing function of the PM isolator. When the total fiber cavity length was about 120 m and the PM fiber segment length was 17 cm, stable mode-locked operation began at a pump power of 820 mW by properly adjusting the angle of the PC and maintained until the pump power reached 900 mW. The pulse train was recorded by the oscilloscope and is shown in Fig. 3(a). The optical spectrum is shown in Fig. 3(b). The central wavelength is 1193 nm and the 10-dB bandwidth is about 8.9 nm. The square-shaped optical spectrum is typical of dissipative soliton mode-locking [21], [22]. The pulse width of the mode-locked laser was measured by an autocorrelator and is shown in Fig. 3(c). A full-width at half-maximum (FWHM) of 65 ps is obtained by fitting the autocorrelation trace with a

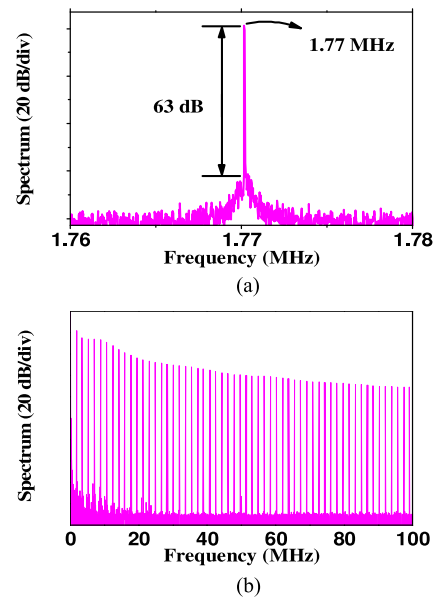


Fig. 4. RF spectrum of the mode-locked fiber laser at  $1.2 \mu\text{m}$  measured (a) around the fundamental repetition frequency and (b) in a range of 0–100 MHz.

Gaussian function and the pulse width is estimated to be  $65/1.4 = 47$  ps. The pulse energy is 1.3 nJ.

The radio-frequency spectrum around the fundamental repetition rate was measured with a resolution of 10 Hz and is shown in Fig. 4(a). The fundamental repetition frequency is 1.77 MHz, which agrees well with the fiber cavity length of 120 m. The signal-to-noise ratio of 63 dB indicates excellent stability of the dissipative soliton mode-locking. The RF spectrum measured in a range of 0–100 MHz is shown in Fig. 4(b).

When the pump power was increased beyond 900 mW, pulse breaking occurred and multi-pulse mode-locking was observed. The pulse number within a burst increased from 2 to 9 as the pump power was increased from 900 mW to 1190 mW. Pulse trains of the multi-pulse mode-locking with 2, 3, and 9 pulses within a burst are shown in Fig. 5(a), 5(b) and 5(c), respectively. The evolution of the multi-pulse mode-locking is depicted in Fig. 5(d), where different colors represent the operation regions with different pulse numbers. The output power of the  $1.2 \mu\text{m}$  mode-locked fiber laser as a function of pump power is also shown in Fig. 5(d). An output power of 11.8 mW was obtained at a pump power of 1190 mW and the energy of the 9-pulse burst is about 6.7 nJ. Further increase of pump power will result in more pulses, which however can not be resolved in our experimental condition. Multi-pulse mode-locked operation, also called burst mode operation, has been commonly observed in NPR mode locked fiber lasers operating in the normal dispersion regime due to overdriven nonlinear polarization evolution [23], [24]. Burst mode operation is an effective way to increase the output power of a mode locked fiber laser [25]. In our experiment, the output power of the 9-pulse mode-locking is about 5 times that of single-pulse operation. The low optical efficiency of the laser is resulted from the high intracavity loss, which is obvious from the high laser threshold, and the fact that the laser works at just slightly over the threshold.

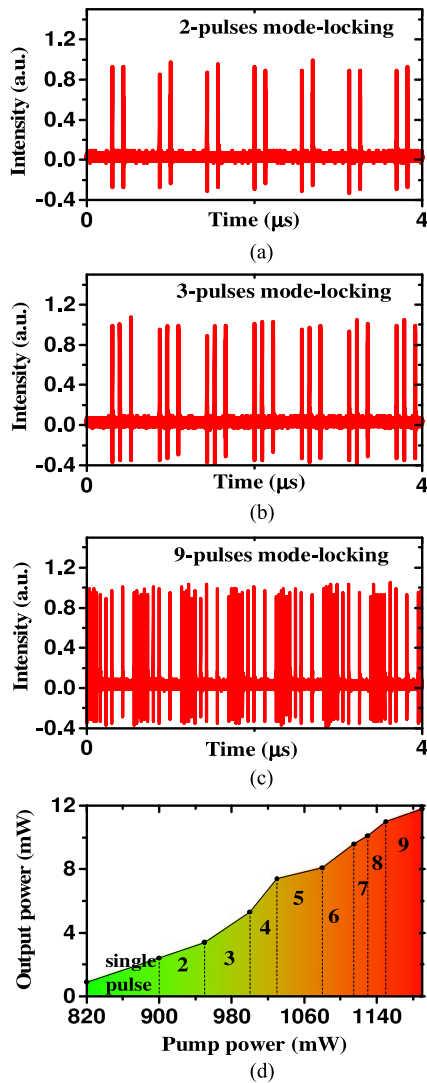


Fig. 5. Typical pulse trains of mode locking states with 2(a), 3(b), and 9(c) pulses. (d) Output power and states of the mode locking as a function of pump power.

Dissipative soliton mode-locking based on NPR is an effective way to achieve low repetition-rate high energy pulses because stable mode-locked operation can be achieved even with a very long fiber cavity. However, in order to balance the interaction of nonlinearity, dispersion, gain, and loss, the intra-cavity filter bandwidth had to be adjusted accordingly. Nevertheless, the bandwidth of an all-fiber Lyot filter can be modified conveniently by changing the length of the PM fiber segment. In order to demonstrate the capability to achieve dissipative soliton mode-locking with lower repetition rates, we increased the cavity length to 170 and 210 m. Stable mode-locked operation was obtained in both cases with PM fiber lengths of 21 and 27 cm, respectively. The pulse widths for the two cases are 52 ps and 164 ps as calculated from the autocorrelation traces shown in Fig. 6(a) and (b), respectively. The experimental results show that the pulse duration increases with increased fiber cavity length. However, the pulse energy for single-pulse mode-locking in both cases remained at 1 nJ level.

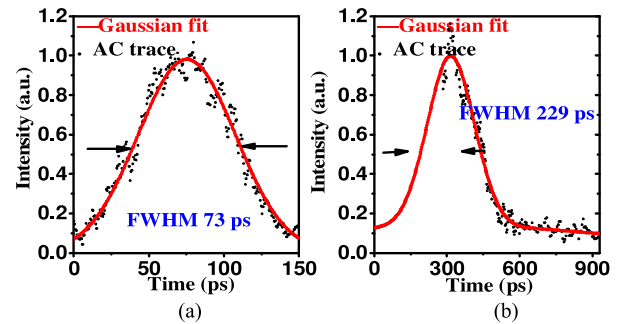


Fig. 6. AC trace of the mode-locked laser with total cavity length of (a) 160 m and (b) 200 m.

#### IV. CONCLUSION

In conclusion, dissipative soliton mode-locking of a Ho<sup>3+</sup>-doped ZBLAN fiber laser at 1.2  $\mu$ m was successfully demonstrated for the first time with the NPR technique and an all-fiber intra-cavity Lyot filter. Single-pulse operation with pulse energy of 1 nJ level and pulse widths of 47 ps, 52 ps, and 164 ps has been obtained with different fiber cavity lengths. Pulse breaking at higher pump powers was observed. At 9-pulse operation, a burst energy of 6.7 nJ was obtained.

#### REFERENCES

- [1] A. M. Wanner *et al.*, "Effects of non-invasive, 1210 nm laser exposure on adipose tissue: Results of a human pilot study," *Laser Surg. Med.*, vol. 41, pp. 401–407, 2009.
- [2] F. Anquez, E. Courtade, A. Sivéry, P. Suret, and S. Randoux, "A high-power tunable Raman fiber ring laser for the investigation of singlet oxygen production from direct laser excitation around 1270 nm," *Opt. Express*, vol. 18, pp. 22928–22936, 2010.
- [3] D. Pliutau and N. S. Prasad, "Simulation studies for comparative evaluation of alternative spectral regions for the sensing of CO<sub>2</sub> and O<sub>2</sub> suitable for the ASCENDS Mission," in *Proc. SPIE*, 2012, pp. 851309–851313.
- [4] A. S. Yusupov, S. E. Goncharov, I. D. Zalevskii, V. M. Paramonov, and A. S. Kurkov, "Raman fiber laser for the drug-free photodynamic therapy," *Laser Phys.*, vol. 20, pp. 357–359, 2010.
- [5] L. Zhang, H. Jiang, S. Cui, J. Hu, and Y. Feng, "Versatile Raman fiber laser for sodium laser guide star," *Laser Photon. Rev.*, vol. 8, pp. 889–895, 2014.
- [6] S. Kivistö *et al.*, "Pulse dynamics of a passively mode-locked Bi-doped fiber laser," *Opt. Express*, vol. 18, pp. 1041–1048, 2010.
- [7] B. H. Chapman *et al.*, "Picosecond bismuth-doped fiber MOPFA for frequency conversion," *Opt. Lett.*, vol. 36, pp. 3792–3794, 2011.
- [8] X. Yang, L. Zhang, H. Jiang, T. Fan, and Y. Feng, "Actively mode-locked Raman fiber laser," *Opt. Express*, vol. 23, pp. 19831–19836, 2015.
- [9] S. Liu *et al.*, "Graphene Q-switched Ho<sup>3+</sup>-doped ZBLAN fiber laser at 1190nm," *Opt. Lett.*, vol. 40, pp. 147–150, 2015.
- [10] G. Zhu, X. Zhu, K. Balakrishnan, R. A. Norwood, and N. Peyghambarian, "Fe<sup>2+</sup>:ZnSe and graphene Q-switched singly Ho<sup>3+</sup>-doped ZBLAN fiber lasers at 3  $\mu$ m," *Opt. Mater. Express*, vol. 3, 2013, Art. no. 1365.
- [11] X. Zhu *et al.*, "Single-frequency Ho<sup>3+</sup>-doped ZBLAN fiber laser at 1200nm," *Opt. Lett.*, vol. 37, pp. 4185–4187, 2012.
- [12] X. Zhu *et al.*, "Watt-level short-length holmium-doped ZBLAN fiber lasers at 1.2  $\mu$ m," *Opt. Lett.*, vol. 39, pp. 1533–1536, 2014.
- [13] N. Photonics, "Method of fusing splicing silica fiber with low-temperature multi-component glass fiber," U.S. Patent 6,705,771, March 16, 2004.
- [14] K. Özgören and F. Ö. İlday, "All-fiber all-normal dispersion laser with a fiber-based Lyot filter," *Opt. Lett.*, vol. 35, pp. 1296–1298, 2010.
- [15] L. Zhao, D. Tang, X. Wu, and H. Zhang, "Dissipative soliton generation in Yb-fiber laser with an invisible intracavity bandpass filter," *Opt. Lett.*, vol. 35, pp. 2756–2758, 2010.
- [16] A. Chong, W. H. Renninger, and F. W. Wise, "Properties of normal-dispersion femtosecond fiber lasers," *J. Opt. Soc. Amer. B*, vol. 25, pp. 140–148, 2008.

- [17] L. Zhang, Y. Feng, and X. Gu, "Wavelength-switchable dissipative soliton fiber laser with a chirped fiber grating stop-band filter," *IEEE Photon. J.*, vol. 5, no. 2, pp. 1500506–1500506, Apr. 2013.
- [18] Z. R. Cai, W. J. Cao, A. P. Luo, Z. B. Lin, Z. C. Luo, and W. C. Xu, "A wide-band tunable femtosecond pulse fiber laser based on an intracavity-birefringence induced spectral filter," *Laser Phys.*, vol. 23, 2013, Art. no. 035107.
- [19] Y. S. Fedotov, S. M. Kobtsev, R. N. Arif, A. G. Rozhin, C. Mou, and S. K. Turitsyn, "Spectrum-, pulsewidth-, and wavelength-switchable all-fiber mode-locked Yb laser with fiber based birefringent filter," *Opt. Express*, vol. 20, pp. 17797–17805, 2012.
- [20] Z. Yan, K. Zhou, A. Adedotun, and L. Zhang, "All-fibre Lyot filters based on 45° tilted gratings UV-inscribed in PM fibre," in *Proc. Adv. Photon. Congr.*, 2012, Art no. BW2E.2.
- [21] A. Chong, W. H. Renninger, and F. W. Wise, "All-normal-dispersion femtosecond fiber laser with pulse energy above 20nJ," *Opt. Lett.*, vol. 32, pp. 2408–2410, 2007.
- [22] L. M. Zhao, D. Y. Tang, and J. Wu, "Gain-guided soliton in a positive group-dispersion fiber laser," *Opt. Lett.*, vol. 31, pp. 1788–1790, 2006.
- [23] A. Haboucha, A. Komarov, H. Leblond, F. Sanchez, and G. Martel, "Mechanism of multiple pulse formation in the normal dispersion regime of passively mode-locked fiber ring lasers," *Opt. Fiber Technol.*, vol. 14, pp. 262–267, 2008.
- [24] X. Liu, "Hysteresis phenomena and multipulse formation of a dissipative system in a passively mode-locked fiber laser," *Phys. Rev. A*, vol. 81, 2010, Art. no. id. 023811.
- [25] H. Kalaycıoğlu *et al.*, "1mJ pulse bursts from a Yb-doped fiber amplifier," *Opt. Lett.*, vol. 37, pp. 2586–2588, 2012.

Authors' biographies not available at the time of publication.